REPORT DOCUMENTATION PAGE

Form Approved
OMB No. 0704-0188

The public reporting burden for this collection of information is estimated to average 1 hour per response, including the time for reviewing instructions, searching existing data sources, gathering and maintaining the data needed, and completing and reviewing the collection of information. Send comments regarding this burden estimate or any other aspect of this collection of information, including suggestions for reducing the burden, to Department of Defense, Washington Headquarters Services, Directorate for Information Operations and Reports (0704-0188), 1215 Jefferson Davis Highway, Suite 1204, Arlington, VA 22202-4302. Respondents should be aware that notwithstanding any other provision of law, no person shall be subject to any penalty for failing to comply with a collection of information if it does not display a currently valid OMB control number.
PLEASE DO NOT RETURN YOUR FORM TO THE ABOVE ADDRESS.

1. REPORT DATE *(DD-MM-YYYY)*	2. REPORT TYPE	3. DATES COVERED *(From - To)*
13-05-2008	Final Report	10/1/05 to 9/30/06

4. TITLE AND SUBTITLE

Final Report> WindSAT Data Analysis for Cal/Val

5a. CONTRACT NUMBER

5b. GRANT NUMBER

N00173-04-1-G024

5c. PROGRAM ELEMENT NUMBER

6. AUTHOR(S)

Ralph C. Foster
Robert A. Brown

5d. PROJECT NUMBER

5e. TASK NUMBER

5f. WORK UNIT NUMBER

7. PERFORMING ORGANIZATION NAME(S) AND ADDRESS(ES)

Applied Physics Laboratory - University of Washington
1013 NE 40th Street
Seattle, WA 98105-6698

8. PERFORMING ORGANIZATION REPORT NUMBER

N/A

9. SPONSORING/MONITORING AGENCY NAME(S) AND ADDRESS(ES)

Office of Naval Research (ONR 322)
875 North Randolph Street
Arlington, VA 22203-1995

10. SPONSOR/MONITOR'S ACRONYM(S)

ONR

11. SPONSOR/MONITOR'S REPORT NUMBER(S)

12. DISTRIBUTION/AVAILABILITY STATEMENT

Unlimited

13. SUPPLEMENTARY NOTES

None

14. ABSTRACT

We investigated the accuracy, capabilities and limitations of surface wind vectors from the first release of WindSAT passive microwave radiometer data using atmospheric boundary layer models and comparisons with NASA QuikSCAT scatterometer winds. Our methods allowed both point by point vector comparisons and integrated, non-local comparisons through derived sea level pressure fields. We found that the preliminary WindSAT winds were surprisingly good and that the combined vector wind and integrated water vapor (CWV) and cloud liquid water (CLW) data would be a valuable product for storms analyses over the ocean if the quality of the wind product could be raised to QuikSCAT levels. For higher winds, WindSAT was comparable to QuikSCAT. In terms of direction, WindSAT vector fields were quite noisy and either got the direction completely wrong or selected the wrong ambiguity about 10% of the time. We found no correlation between the bad vectors and either CLW or CWV. We concluded that incorporating sea-level pressure into the surface wind retrievals has promise as a means to improve the WindSAT model function.

15. SUBJECT TERMS

WindSAT, satellite ocean vector winds, passive microwave remote sensing, sea-level pressure retrieval, planetary boundary layer

16. SECURITY CLASSIFICATION OF:			17. LIMITATION OF ABSTRACT	18. NUMBER OF PAGES	19a. NAME OF RESPONSIBLE PERSON
a. REPORT	b. ABSTRACT	c. THIS PAGE	UU	25	Dr. Peter Gaiser
U	U	U			**19b. TELEPHONE NUMBER** *(Include area code)* 202-767-8253

Standard Form 298 (Rev. 8/98)
Prescribed by ANSI Std. Z39.18

Final Report: WindSAT Data Analysis for Cal/Val

PI: Ralph C. Foster
Applied Physics Laboratory
University of Washington
1013 NE 40th St.
Seattle, WA, 98105-6698

Co-PI: Robert A. Brown,
Department of Atmospheric Sciences
Box: 351640
University of Washington
Seattle, WA. 98195-1640

Summary: We investigated the accuracy, capabilities and limitations of surface wind vectors from the first release of WindSAT passive microwave radiometer data using atmospheric boundary layer models and comparisons with NASA QuikSCAT scatterometer winds. Our methods allowed both point by point vector comparisons and integrated, non-local comparisons through derived sea level pressure fields. We found that the preliminary WindSAT winds were surprisingly good and that the combined vector wind and integrated water vapor (CWV) and cloud liquid water (CLW) data would be a valuable product for storms analyses over the ocean if the quality of the wind product could be raised to QuikSCAT levels. The distribution of WindSAT windspeeds were biased compared to that from QuikSCAT, with too few winds in the range $U_{10}^N < 5\,m\,s^{-1}$; too many winds in the range $5\,m\,s^{-1} < U_{10}^N < 8\,m\,s^{-1}$; too few winds in the range $8\,m\,s^{-1} < U_{10}^N < 12\,m\,s^{-1}$. For higher winds, WindSAT was comparable to QuikSCAT. In terms of direction, WindSAT vector fields were quite noisy and either got the direction completely wrong or selected the wrong ambiguity about 10% of the time. Most of these bad vectors had windspeeds $U_{10}^N < 8\,m\,s^{-1}$. About 37% of the bad vectors had unselected ambiguities that better matched the local meteorology. We found no correlation between the bad vectors and either CLW or CWV. We concluded that incorporating sea-level pressure into the surface wind retrievals has promise as a means to improve the WindSAT model function.

Introduction

Surface wind[1] is a crucial factor in the calculation of the air-surface flux of heat and water vapor. It is important in other air-sea interaction fluxes such as oceanic stress (momentum flux) and gas exchange. The state-of-the-art methods of calculating these fluxes always contain the surface wind as a direct factor (squared in the case of surface stress). A typical 10% error in climate record surface winds can be significant to climate models (Foster and Brown, 1994a).

The only current sources of surface wind data are: general circulation model (GCM) products, oceanic surface winds from ERS2 (1996-), QuikScat (1999-) and possibly WindSat (2003), surface wind speeds from several other microwave satellite sensors and very sparse surface measurements from ships and buoys. Marine Planetary Boundary Layer (PBL) winds are measured well by the satellite scatterometers. However, the failure of the ADEOS-II satellite and SeaWinds scatterometer in 2003 means that there will be a gap in scatterometer winds. The ESA ASCAT scatterometer has much coarser resolution than QuikSCAT and has substantially less coverage. To use satellite winds to track storms (mid-latitude to hurricanes) and the surface wind features of their associated frontal boundaries, the temporal resolution needs to be very high, once/day. For instance, this is short of adequate even with the large (1800-km swath, 12.5-km resolution) coverage of QuikScat. One hope is that WindSAT can help fill this void. However, it uses new technology and its performance must be validated.

WindSAT Measurements

Passive microwave radiometers measure emission (brightness temperature) from the sea surface. Because this signal varies due to the non-homogeneity in the waves, the possibility exists that wind direction might be extracted from the polarization information in the radiometer signal (e.g. Poe and St Germain, 1998). WindSat serves as the 'proof of concept' of this idea.

Wind speed retrieval from passive radiometers is well established, for example from SSM/I data (Wentz, 1997). However, the directional information in the microwave emission is contained in a weaker and more difficult to measure part of the signal, the polarization, that is also affected, for example, by the salinity, sea surface temperature and the presence of foam. Furthermore, clouds and precipitable water in the atmosphere will also affect the measured microwave brightness temperatures (related to the surface emission). Hence, establishing the accuracy and utility limits of the retrieved vector winds presents a challenge. The retrieved winds must be compared to averaged in situ

---

[1] In this report, when we refer to winds or surface winds we mean the neutral-equivalent ten-meter wind, U_{10}^N, which is the virtual wind speed at 10 m above the sea surface that, in neutral stratification, would exert the same stress as the actual wind.

winds in a manner that properly accounts for the effects of spatial averaging, planetary boundary layer dynamics and other processes.

Wentz (1992) investigated the suggestion that a measurable directional signal exists in passive microwave brightness temperatures and found that a useable signal was present in SSM/I data. (Note, however, that the SSM/I studies are restricted to combinations of horizontal and vertical polarization.) A theoretical model for the variation of all four Stokes polarization parameters as a function of relative look direction was constructed by Poe and St Germain (1998) who predicted very similar directional signals as those estimated from data by Wentz (1992). A more detailed study combining SSM/I, TRMM and QuikSCAT data was performed by Meissner and Wentz (2002) who found that the directional signal was absent for winds less than 6 m s^{-1} and about half the amplitude of that found in Wentz (1992) and Poe and St Germain (1998) for winds in the range 6 - 10 m s^{-1}. From 10 – 14 m s^{-1} the new observations agreed with the earlier results. Meissner and Wentz (2002) showed that the apparently larger directional signal in Wentz (1992) was due to a correlation of assumed atmospheric properties (column integrated water vapor and liquid water) and relative look direction between the radiometer and wind. This effect was removed in the 2002 study by combining SSM/I and TRMM because the former are in polar orbits while the latter is in an equatorial orbit which allows winds to be measured with one satellite and water properties with the other at a different look angle.

These studies suggest that the chances of obtaining good wind vectors from a passive radiometer are best for winds above 10 m s^{-1} in cloud-free conditions. Near clouds or precipitation the quality may degrade. There is likely useful directional information in the intermediate wind regime (6-10 m s^{-1}) but this must be carefully checked. In particular, clouds or rain may reduce the detectability in this wind regime. This intermediate speed regime is the most common over the ocean. Finally, the directional signal at low winds may be too small to detect. For this regime, cloud free conditions should maximize the chances of finding good vectors. Of course, defining a wind direction in light winds can be problematic and averaging and representativeness (e.g. coherent structure effects) errors play an important role. For winds less than 10 m s^{-1} direction retrieval may hinge on contributions from the 3rd and 4th Stokes parameters. There is little chance of retrieving winds in regions where it is raining.

Methodology

Cal/Val of WindSat depends on obtaining a compatible wind data set. This is not an easy thing to do, as most global surface wind sources have significant limitations (Brown, 2002, 2001, 2000; Foster and Brown, 1994a). The best source of compatible data will be from satellite scatterometer augmented with good PBL models.

We have also developed models and procedures that account for important effects of storm dynamics and other PBL processes on surface winds. The gradient wind correction is crucial in tropical cyclones or other regions of significant curvature (Patoux and Brown, 2002). Foster et al. (1999) showed that shear induced by horizontal temperature

gradients in the boundary layer makes a significant contribution to the error in scatterometer wind retrievals that increases with the strength of the gradient and becomes very strong in frontal zones. Foster and Levy (1998) showed that combined effects of PBL coherent structures (rolls) and baroclinic shear on the magnitude and direction of the surface wind vector are stronger than the sum of either effect acting in isolation.

A unique tool that we use in our analyses is a two-layer similarity PBL model that relates the basic surface data (pressure, temperature, etc.) to the surface wind vector and surface fluxes (Brown, 1974). The model includes the mean effects of PBL rolls, stratification, baroclinic shear and flow curvature and has been found to agree very well with the scatterometer winds. It can also be used in an "inverse" mode to derive sea level pressure (SLP) fields from scatterometer wind swaths (Brown and Levy, 1986; Patoux et al., 2003; Patoux et al., 2008). These pressure fields have proven to be highly accurate and to contain small-scale details missed in the standard global analyses (Patoux, 2003; Patoux et al., 2008). We also have a high-order non-linear model for the structure and dynamics of the PBL rolls (Foster, 1996; 2005). Recent studies sponsored by the IPO have shown that this model agrees well with high-resolution PBL winds retrieved from an airborne Doppler Lidar (Foster and Brown, 2004). This study has demonstrated that rolls in typical conditions induce km-scale +/- 2 m s^{-1} variation in surface wind speed, which must be considered to be a limiting factor wind validation.

We use the swath data from both WindSAT and QuikSCAT to compare with other wind data and to analyze marine storms. From these swaths, we construct sea-level pressure (SLP) fields, which allows a unique methodology for evaluating both speed and direction and will allow the use of surface pressure observations to validate the overall performance of WindSAT winds. The SLP field represents a large-scale quantity that is the best dynamical fit to the purely locally-derived wind vectors. The direct PBL model can then be used to derive a "model" wind vector field, which is an optimally smoothed comparison data set.

It must be emphasized that because the SLP is a global, integrated quantity, it is fairly insensitive to localized patches of bad vectors; the much larger number of good vectors sufficiently defines the overall pressure pattern that the impact of the smaller number of bad vectors is minimized (Patoux and Brown, 2001; Patoux et al., 2008). Furthermore, the SLP gradients defined by the swath winds are a very sensitive measure of the accuracy of the satellite surface wind gradients. This is very important when evaluating surface winds from WindSAT. The baseline validation data set is QuikSCAT. Chelton et al. (2006) showed that QuikSCAT winds are a highly accurate representation of the actual surface wind field and that they contain accurate mesoscale structure that is *not* always present in the ECMWF surface wind analyses. Patoux et al. (2008) showed that the QuikSCAT-derived pressure fields are consistent with the QuikSCAT surface winds and that the SLP contains accurate mesoscale information that is often missing in ECMWF. A basic goal for WindSAT should be to match the performance of QuikSCAT in terms of accurately capturing the mesoscale surface wind information that is missing in ECMWF (Chelton, et al., 2006).

We use the SLP fields derived from the inverse PBL model to identify the "bad" vectors in the swaths These bad vectors may indicate problems with either the model function or the ambiguity selection methodology.

Wind Speed Analysis

As an example, consider Figure 1, which show segments of QuikSCAT and WindSAT swaths over the Pacific Ocean on the morning of 1 Sep, 2003 near a fairly deep storm. Even allowing for the two hour time difference between the swaths, there are noticeable differences in the wind fields, especially in the western edges of the WindSAT swath. In general, for winds in the 8 to 12 m s^{-1} range that cover most of the overlap regions, the QuikSCAT winds are generally stronger. Of interest is that the general sense of the wind directions is very similar and both fields capture the frontal region in the south-eastern portion of the swaths.

Figure 2 shows the distribution of surface winds speeds poleward of 20° for both QuikSCAT and WindSAT as well as the surface wind speeds derived from the retrieved surface pressures. Evidently the WindSAT predicts too few winds below 5 m s^{-1}, too many winds between $5 < U_{10} < 8$ m s^{-1}, too few winds in $8 < U_{10} < 12$ m s^{-1}, but is comparable to QuikSCAT in the range $12 < U_{10} < 15$ m s^{-1}. The sample size was too small to assess the higher wind regimes. Note that the general trend of the SLP-derived surface winds is to correct for these biases back towards the QuikSCAT wind distribution. This reflects the general insensitivity of SLP retrievals to the bad vectors.

Figures 3 and 4 show a set of SLP retrievals from four morning swaths from each satellite on the morning of 1 Sep, 2003. Clearly the QuikSCAT-derived SLP are in excellent agreement with the ECMWF analysis, which is plotted in dashed lines. Note that there appears to be more meso-scale detail in the QuikSCAT SLP than in ECMWF. Figure 3 shows the equivalent comparison for WindSAT. Most noticeable is the greatly reduced coverage in WindSAT. Many interesting structures captured by both ECMWF and QuikSCAT are missed by WindSAT. However, the overall sense of the WindSAT SLP is still fairly good, especially in the southern hemisphere. For example, it does a reasonable job of capturing the pressure gradients in the 03:31 swath. Note however that WindSAT does a very poor job of resolving the low center near 45N and 175W.

A fairly simple way to summarize these comparisons is to average the pressure along latitude lines and compare it to the averaged ECMWF analysis. We restrict this comparisons to latitudes poleward of 20° latitude since that is the region where we have the highest confidence in the SLP retrievals. Figure 5 shows an example of a typical QuikSCAT swath and Figure 6 shows a good WindSAT swath. There is no apparent difference in correlation with ECMWF between the hemispheres. Note that even though the pressure gradients are very comparable, QuikSCAT often resolves sharper gradients than ECMWF. The WindSAT comparison is very different (e.g, Figure 6). We find that the agreement is generally better in the southern hemisphere, perhaps because this is the stormier and higher wind late-winter, early-spring hemisphere. WindSAT SLP implies

higher gradients over ridges, which is consistent with the high bias in the lower wind speed regime.

The results are summarized in Table 1 in terms of the pressure standard deviation and correlation relative to ECMWF. QuikSCAT correlations are near or above 0.9 and the rms is near or below 3 mb, except for the 07:12 swath. In the southern hemisphere, WindSAT is also highly correlated with ECMWF, but with generally higher rms. Note that the WindSAT 08:35 swath, which covers a region similar to the QuikSCAT 07:12 swath, also has a higher rms than the others. However, WindSAT is indicating a very different pressure pattern near Tazmania than either ECMWF or QuikSCAT, which appears to capture the deep low near 60° S fairly well. Overall we find that the indications from the SLP fields and the wind distributions are consistent. Hence, correcting these biases will be crucial if WindSAT-type data are to be used in data assimilation.

Table 1: Summary of retrieved SLP comparison with ECMWF analyses.				
Time	Nothern Hemisphere		Southern Hemisphere	
	σ (mb)	R	σ (mb)	R
QuikSCAT				
02:09	0.45	0.97	3.00	0.97
03:50	1.06	0.98	2.16	0.99
05:31	2.31	0.95	3.61	0.99
07:12	1.39	0.87	8.43	0.95
WindSAT				
03:31	4.56	0.65	2.65	0.98
05:13	5.04	0.44	2.48	0.95
06:55	6.90	-0.06	5.83	0.93
08:35	2.73	0.84	10.70	0.96

Direction Analysis

One value of the surface pressure retrievals is that they allow a simple consistency check on the wind directions. The pressure retrievals are fairly insensitive to localized regions of bad winds. We assume that the mean surface wind flow will be constrained by the large-scale flow indicated by the surface pressure field. We identify "bad" as those vectors whose directions differ from the SLP-derived surface winds by more than 35°. This threshold is arbitrary, but it proved to be a reliable, objective indicator.

We found no correlation between directional error and either cloud liquid water or cloud water vapor products from WindSAT. Poleward of 20° latitude we found that ~11% of the WindSAT vectors were bad. Of this 11%, 37% (representing about 4% of the total number of bad vectors) had unselected ambiguities that were in better agreement with the SLP fields. Typically , compared to the selected bad vector, the better unselected ambiguity had nearly the same wind speed, but a 60° to 120° rotation. This indicates that incorporating SLP retrievals in the ambiguity selection process could be of major benefit in future model function development.

Figure 7a compares the overall wind speed distribution with the wind speed distribution of the bad vectors. Most of the bad vectors were lower than 8 m s^{-1} and 70% were lower than 5 m s^{-1}. Thus, in both speed and direction, the low wind regime in WindSAT is problematic. Figure 7b shows the distribution of the directional differences between the SLP-derived directions ("model" directions) for just the bad vectors. We we apply the "SLP filtering" of wind directions in those cases where there is a better ambiguity, we find a significant narrowing of the directional error distribution.

A more common representation of directional error vs. wind speed is shown in Figure 8. Note that WindSAT vectors have had the SLP directional filtering applied, so we are comparing the best ambiguity rather than the selected ambiguity. Overall, the comparison with QuikSCAT is surprisingly good. The mean of the directional difference is near zero and the standard deviations have very similar dependence on wind speed.

Three Examples of the Potential in the WindSAT Data

We present two examples from the preliminary WindSAT data release that illustrate how WindSAT winds can be used to create a useful synoptic picture of the lower troposphere (in particular surface pressure fields). These examples reveal how our UWPBL model can help correct certain ambiguity selection problems, and how a combination of WindSAT products can provide useful mesoscale information in frontal areas and tropical convective regions. We also present an example from the Arabian Sea, which is a region of extreme PBL conditions where all remote sensors and standard PBL models perform poorly.

DOUBLE FRONTS

The first example is a WindSAT swath cutting through a mature midlatitude cyclone in the Southern Hemisphere. Figure 9b shows the WindSAT-derived pressure field (colors and solid contours) overlaid on the ECMWF surface pressure field from one hour later. The white box is blown up Figure 9a to outline the presence of a "double front", visible in the wind field as two distinct lines of convergent winds. Figure 9a also shows a region (17°E 36°S) where the WindSAT model function has obviously selected a number of wrong ambiguities. In such cases our model, by calculating the surface pressure field at the scale of the swath and then calculating a new set of surface wind vectors from this pressure field, allows us to select an ambiguity that is most likely closer to the real wind vector. In general, the new set of surface winds agree with the original field except where there are obvious errors in these fields. The surface pressure analysis serves as a self-contained low pass filter. This is very useful since storms analyses often rely on differential fields such as divergence and vorticity.

For example, the WindSAT divergence field calculated with the erroneous wind vectors is misleading (Fig. 10a, in which we have plotted only 5% of the wind vectors for clarity). The southwest convergence band is present but the "second" front does not appear. Figure 10b shows that in the problematic region, the retrieval algorithm has erroneously picked the first ambiguity (black wind vectors) whereas the second

ambiguity (red) would be a better choice in that case. After running our PBL model and choosing the best ambiguity, the resulting divergence field clearly shows two bands of convergence corresponding to the two fronts (Fig. 10c). Note that the fact that the maximum convergence occurs behind the front is consistent with previous observations and modeling of frontal development.

The value of coincident cloud and wind data is demonstrated in Figure 10d, in which the presence of two fronts is confirmed in the WindSAT cloud liquid water (CLW) data. Figure 10d shows the divergence contours overlaid on CLW depth. A primary maximum can be observed ahead of the northeast front and a secondary maximum ahead of the southwest front. This is also consistent with frontal evolution – clouds form "ahead" of the front. Note that the primary CLW maximum corresponds to the front that was not captured well by the uncorrected wind field. Without a detailed analysis of the boundary layer dynamics this inconsistency would have led to an erroneous analysis.

ROTATING CONVECTIVE STORM

The second example is a convective cell over the western Pacific Ocean (13°N) with both strong convergence and vorticity. Figure 11a shows the selected WindSAT wind vectors (in black) and reveals numerous ambiguity removal problems, revealed as 180° shifts. Figure 11b shows the wind vectors after using our PBL model to select a better ambiguity.

It is interesting to note that in both of these two examples, the ambiguity problem occurs with primarily meridional wind vectors; this suggests that the retrieval algorithm might be less skilled for along-swath-blowing winds.

This example presents an example where WindSAT appears to retrieve vectors in conditions where QuikSCAT failed. Figure 12a-b compare the corrected WindSAT winds with QuikSCAT winds from 15 minutes later. Blue circles indicate QuikSCAT rain contamination. Figure 12c shows the resulting divergence pattern and Fig. 12d shows CLW depth with overlaid divergence contours. All plots are exhibit corresponding features; note the other convective cell in the southwest corner of the plot with matching convergence and cloud formation. The CLW indicates thick clouds in the region of strong convergence, where QuikSCAT was unable to retrieve winds and misses much of the convergence. WindSAT data could be used to study the development of such convective systems in the Tropics, an area where measurements are scarce and our understanding of the interactions between mesoscale systems and the synoptic flow is limited.

ARABIAN SEA

The Arabian Sea region presents a difficult test for PBL theory, modeling and remote sensing. This is a region of frequent deep convection in the ocean that leads to relatively very cool SST in the coastal zone (out to 200-300 km) during monsoonal periods where warm, dry (and frequently dusty) air blows off-shore. Ship and buoy observations have found essentially calm sea surfaces (no waves) underneath winds of ~10 ms^{-1} at 15 m and

T_{air} – SST ~ 1.5°. I.e., essentially complete decoupling between 15 m and the sea surface in stable stratification – Monin-Obukhov similarity has broken down. This is a region where, for example, SSM/I and QuikSCAT wind speed differences reach a maxima. Our colleague, Prof. Shuyi Chen of University of Miami, has run the MM5 mesoscale model in this region and found that its PBL representation is a poor match to the limited data.

Figure 13 shows the WindSAT SST in the Arabian Sea with WindSAT and QuikSCAT wind vectors overlayed. It is readily apparent that this is a region of great difficulty for WindSAT. However, given the observed strong decoupling we cannot assume that QuikSCAT is retrieving the correct winds. The coincident cloud and SST data on WindSAT will provide additional insight into the PBL dynamics in this region. In particular, these data will aid in determining the stratification of the PBL. Our PBL model yields significant differences in surface wind vectors depending on the stratification. A combined analysis of WindSAT and QuikSCAT data in this region should prove useful to modelers and developers of PBL parameterizations trying to simulate the complex dynamics of this region.
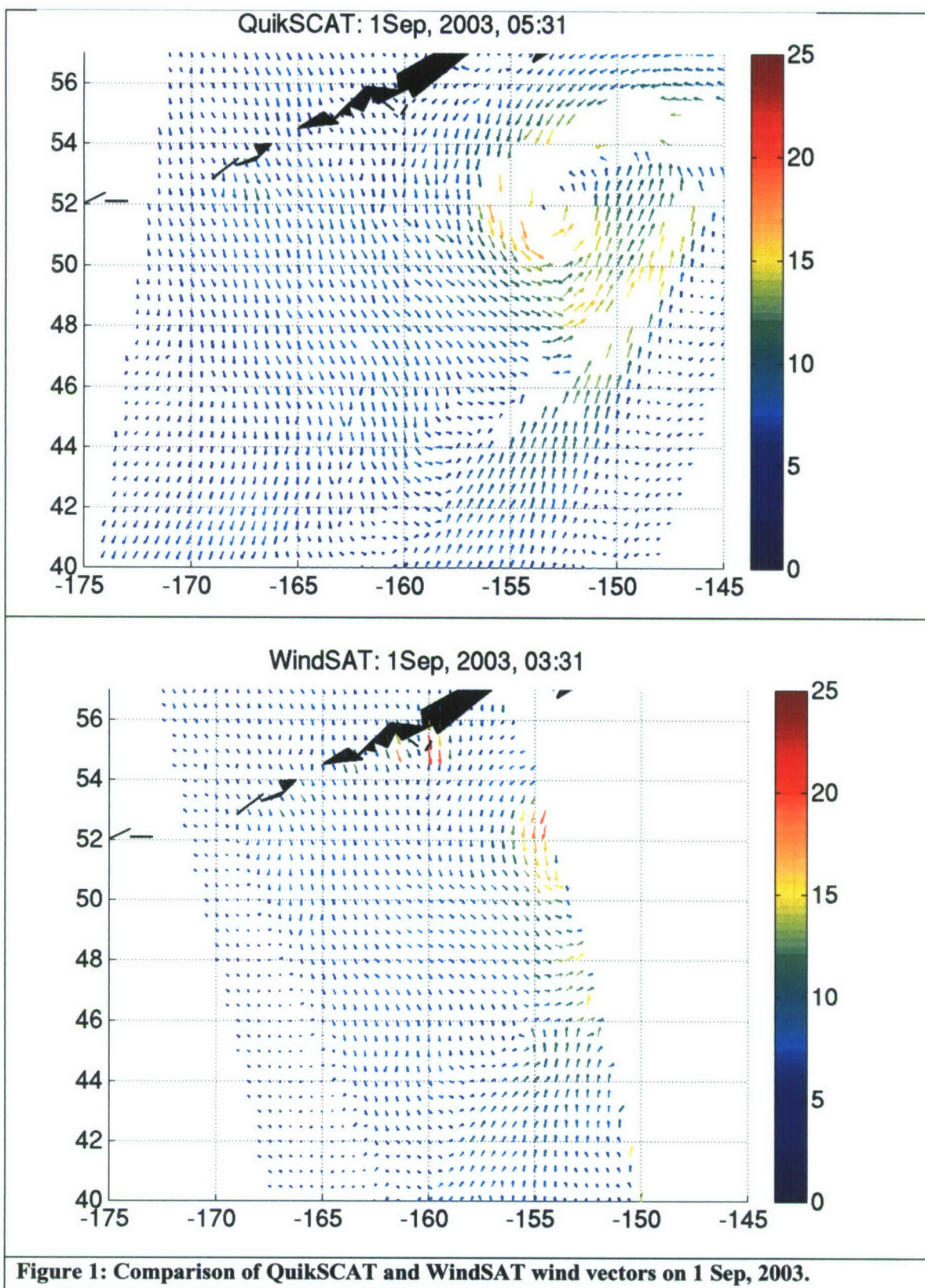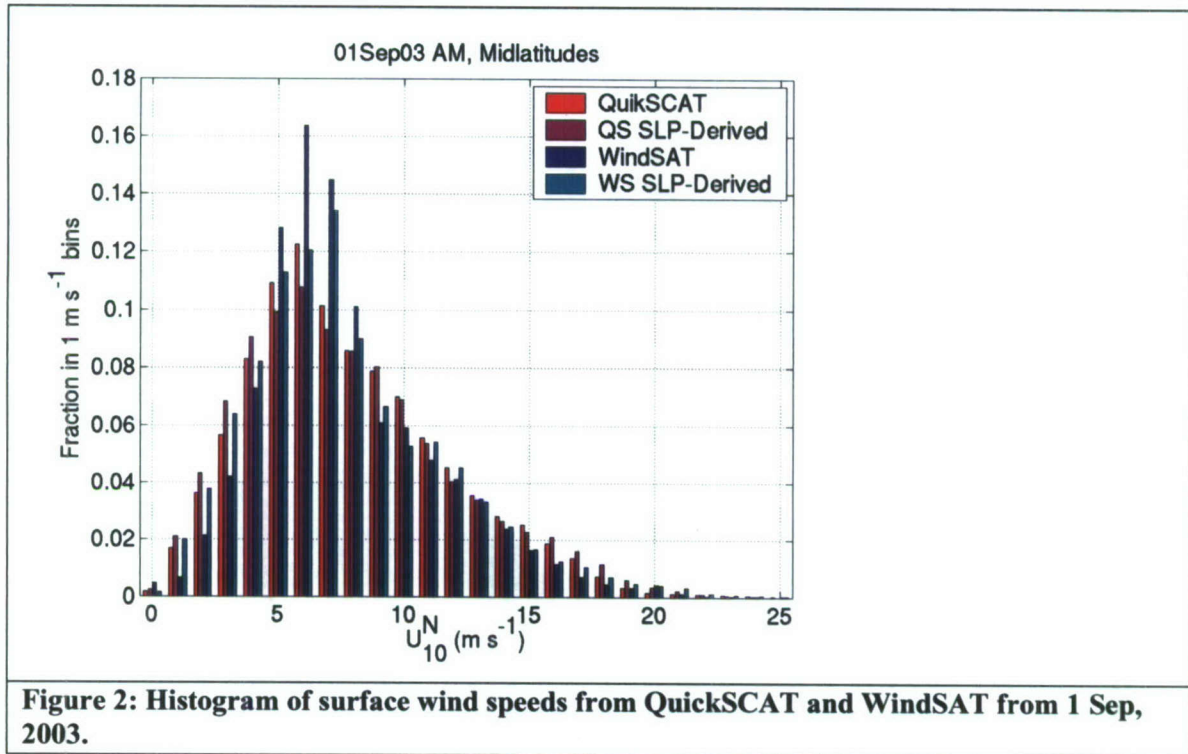
Presentations

"WindSAT Cal/Val via SLP Retrievals", R.C. Foster, J. Patoux & R.A. Brown, WindSat Cal/Val and Science Team meeting , 17-18 November, 2004.
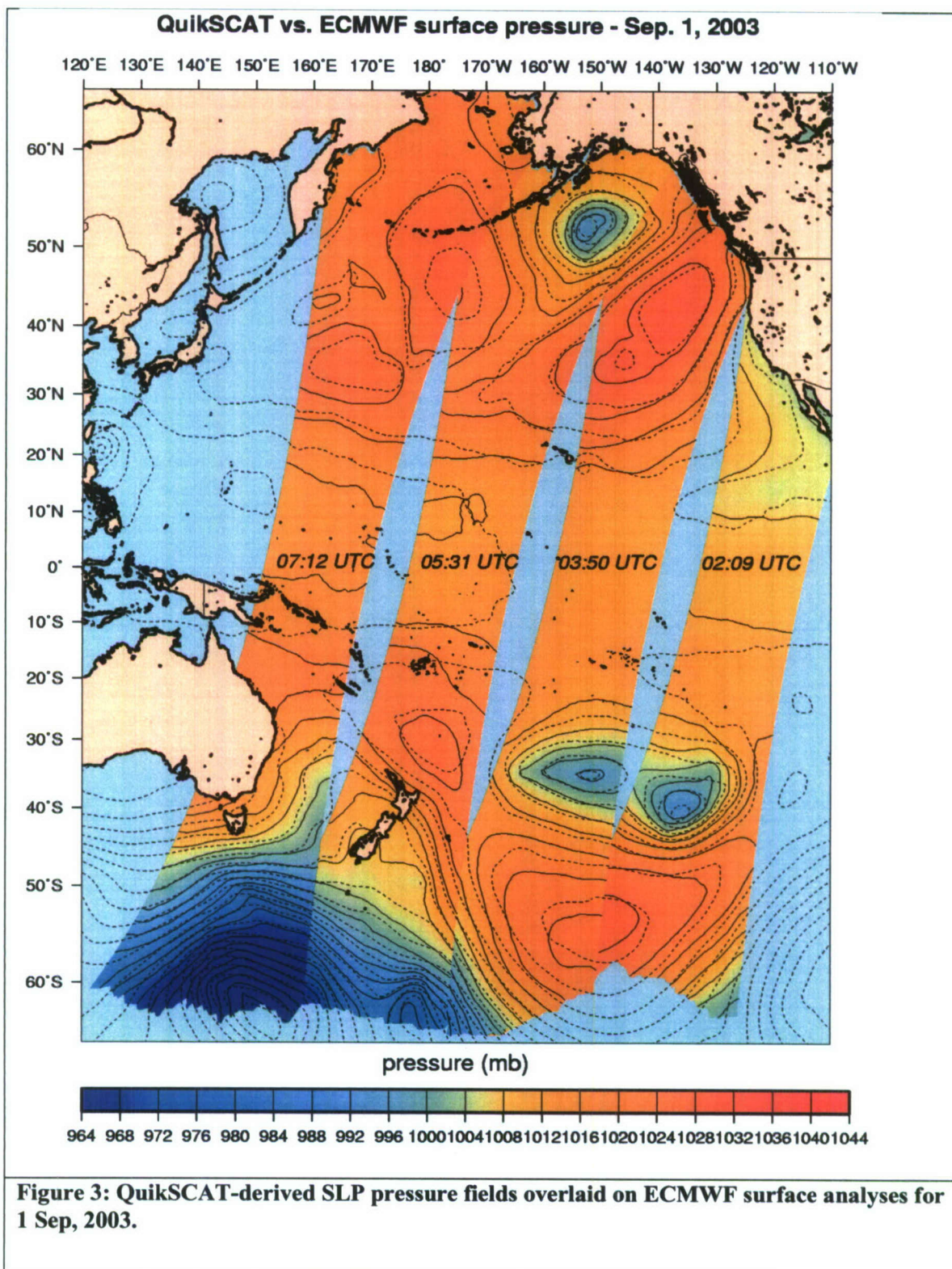
Conclusions

Our analysis of the preliminary WindSAT data was highly encouraging. For the reasons discussed in the WindSAT Measurements section, our expectations were that the surface wind fields would be of significantly lower quality than scatterometer winds. The speed and direction errors are consistent with what would be expected from the analysis of Meissner and Wentz (2002). However, the WindSAT winds show significant promise assuming that the model function errors identified here can be reliably corrected. We suggest that SLP fields derived from the surface winds would be of enormous value in assessing and improving the WindSAT wind data. The combined surface wind, SST and column water vapor and liquid water data set may prove of great value in storms analyses.

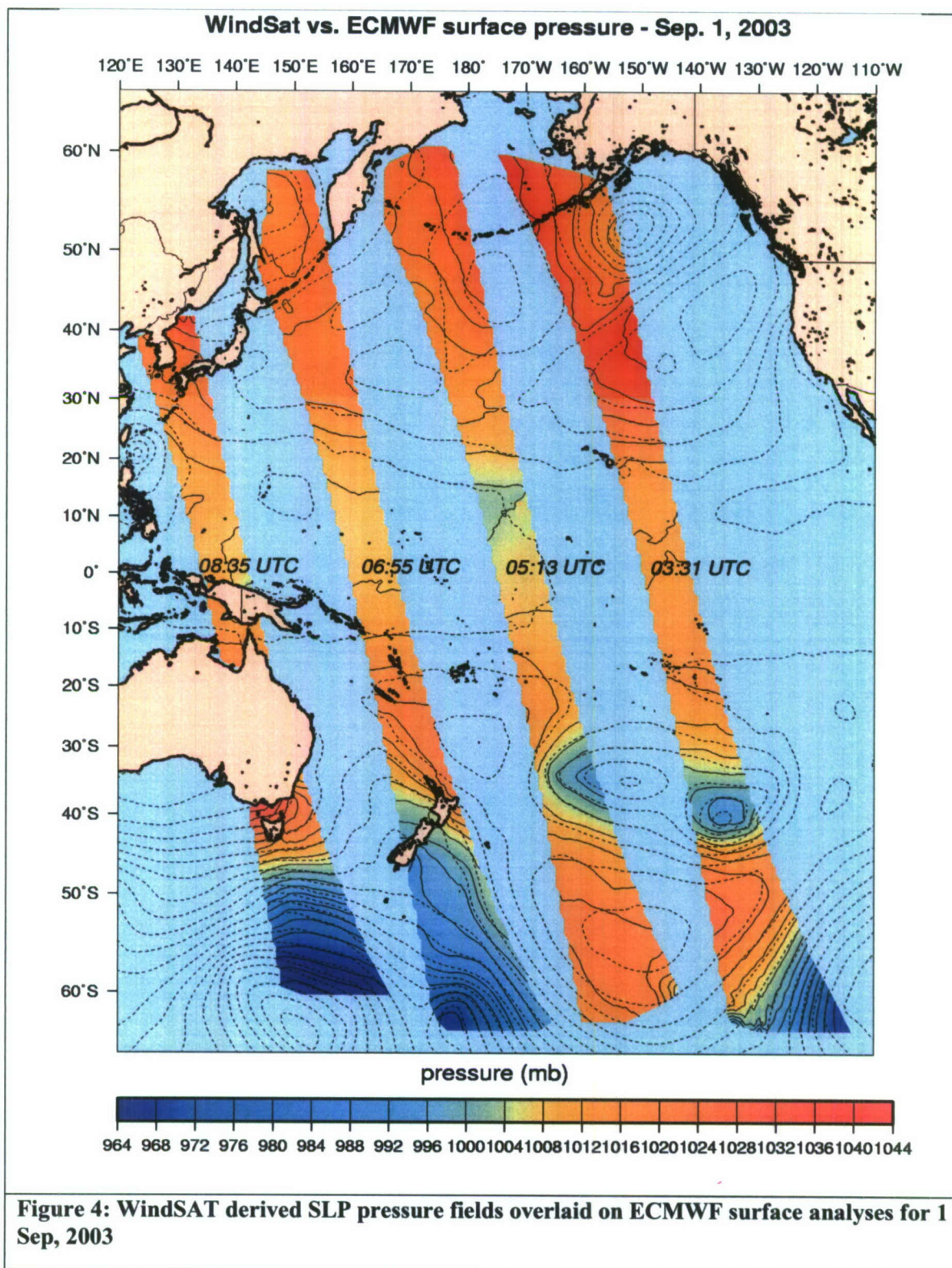Figure 1: Comparison of QuikSCAT and WindSAT wind vectors on 1 Sep, 2003.

Figure 2: Histogram of surface wind speeds from QuickSCAT and WindSAT from 1 Sep, 2003.

Figure 3: QuikSCAT-derived SLP pressure fields overlaid on ECMWF surface analyses for 1 Sep, 2003.

WindSat vs. ECMWF surface pressure - Sep. 1, 2003

08:35 UTC   06:55 UTC   05:13 UTC   03:31 UTC

pressure (mb)

964 968 972 976 980 984 988 992 996 1000 1004 1008 1012 1016 1020 1024 1028 1032 1036 1040 1044

Figure 4: WindSAT derived SLP pressure fields overlaid on ECMWF surface analyses for 1 Sep, 2003

Figure 5: Typical QuikSCAT pressure fields. (a) Northern Hemisphere; (b) latitudinal average; (c) Southern Hemisphere; (d) Latitudinal Average.

15

Figure 6: Good WindSAT pressure fields. (a) Northern Hemisphere; (b) latitudinal average; (c) Southern Hemisphere; (d) Latitudinal Average.

Figure 7:.(a) Distribution of WindSAT wind speeds for all vectors and for just those vectors identified as "bad" by the SLP-filter method. (b) Distribution of directional differences between WindSAT vectors and those derived from the retrieved SLP field.

Figure 8 Dependence of directional difference between satellite surface wind vectors and SLP-derived surface wind vectors on surface wind speed. Note that the WindSAT vectors have the SLP-filtering applied.

(a) WindSat winds (Sep. 1st, 2003 - 05:00 UTC)

(b) WindSat-derived (solid and colors) vs. ECMWF (dashed) slp

Figure 9: (a) WindSAT wind vectors from 1 Sep, 2005, 0500 UTC. (b) ECMWF sea-level pressure analysis from 1 Sep, 2005, 0600 UTC with WindSAT-derived seal-level pressures overlaid. White box shows region detailed in Figure 2.
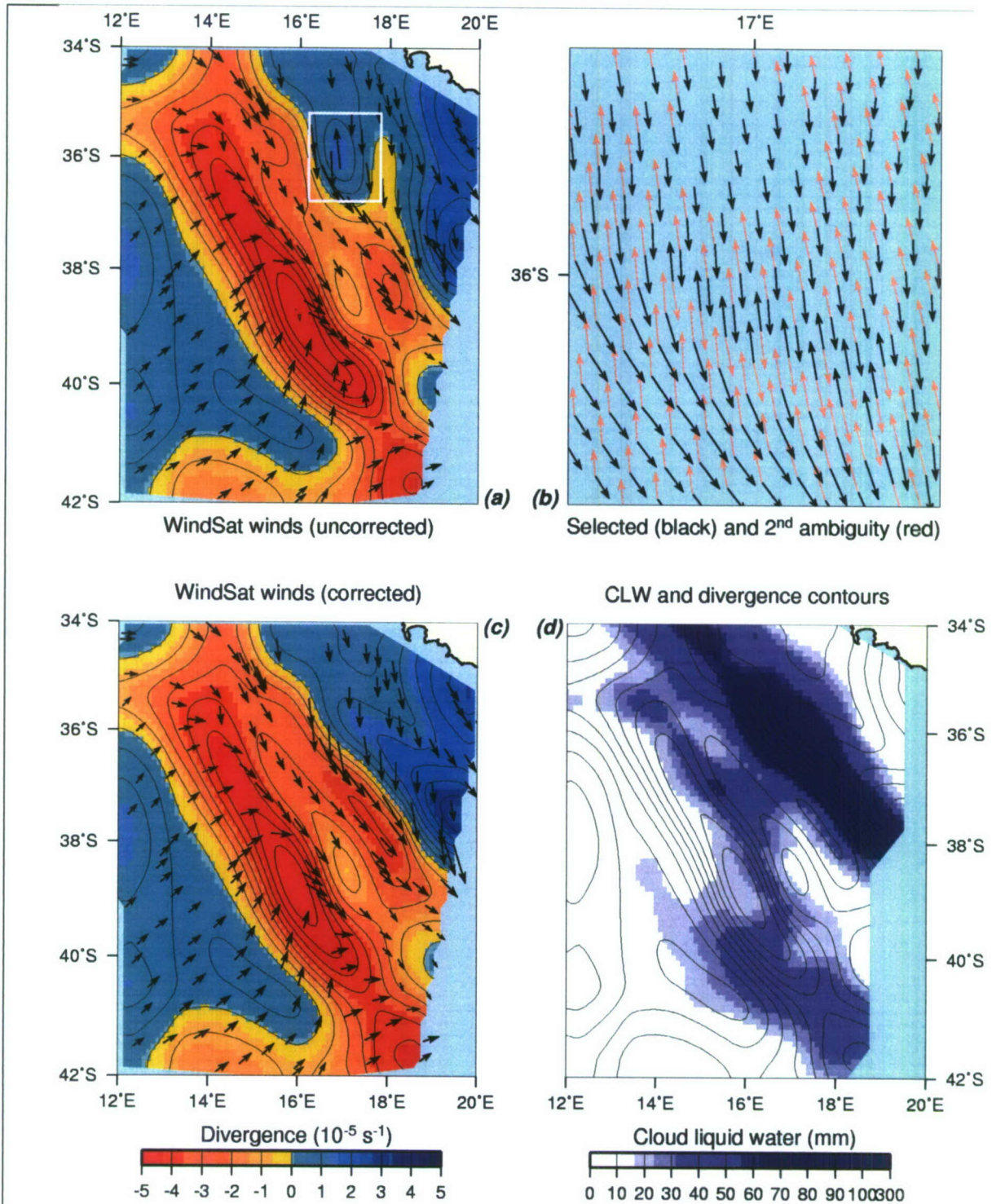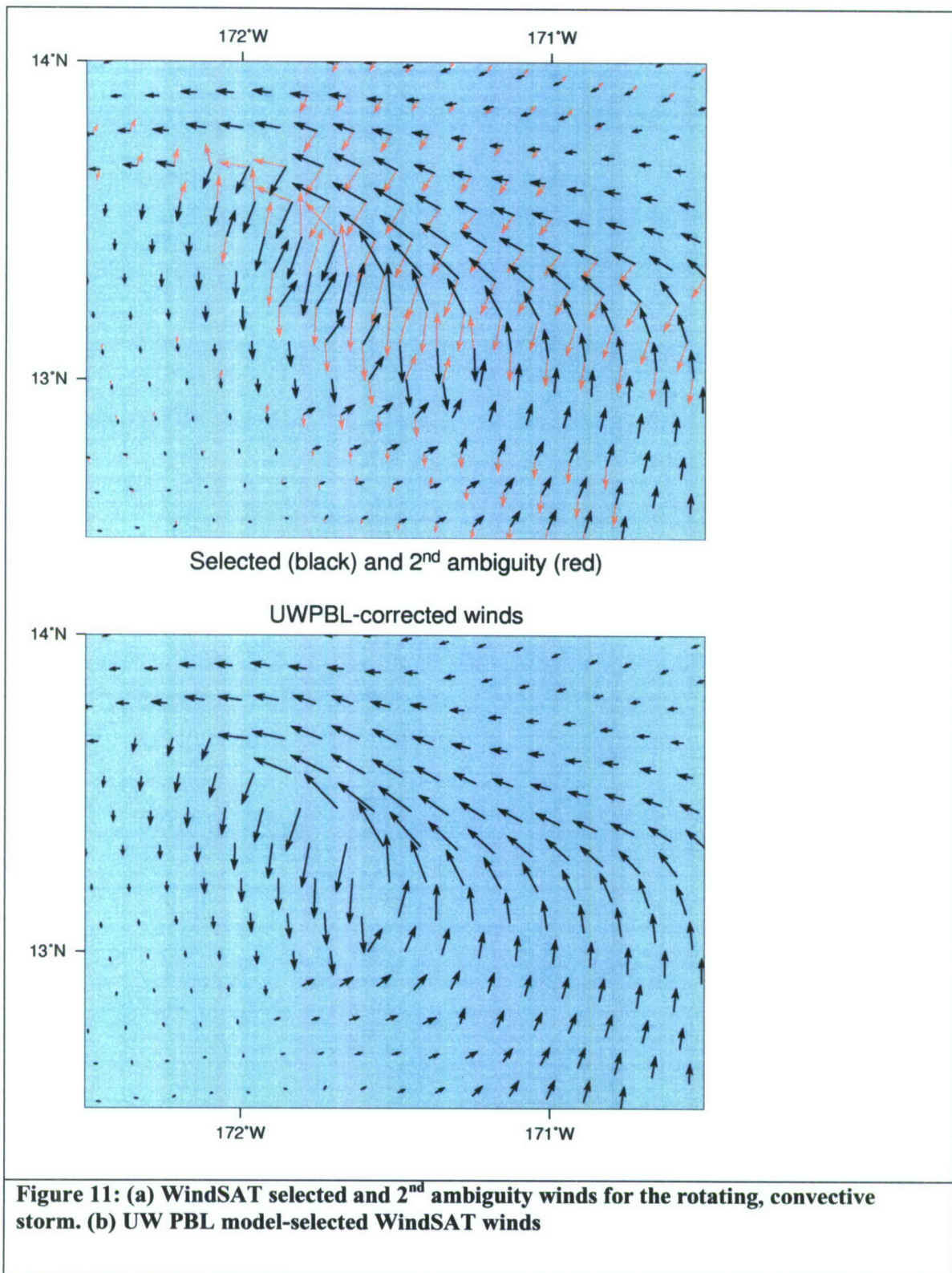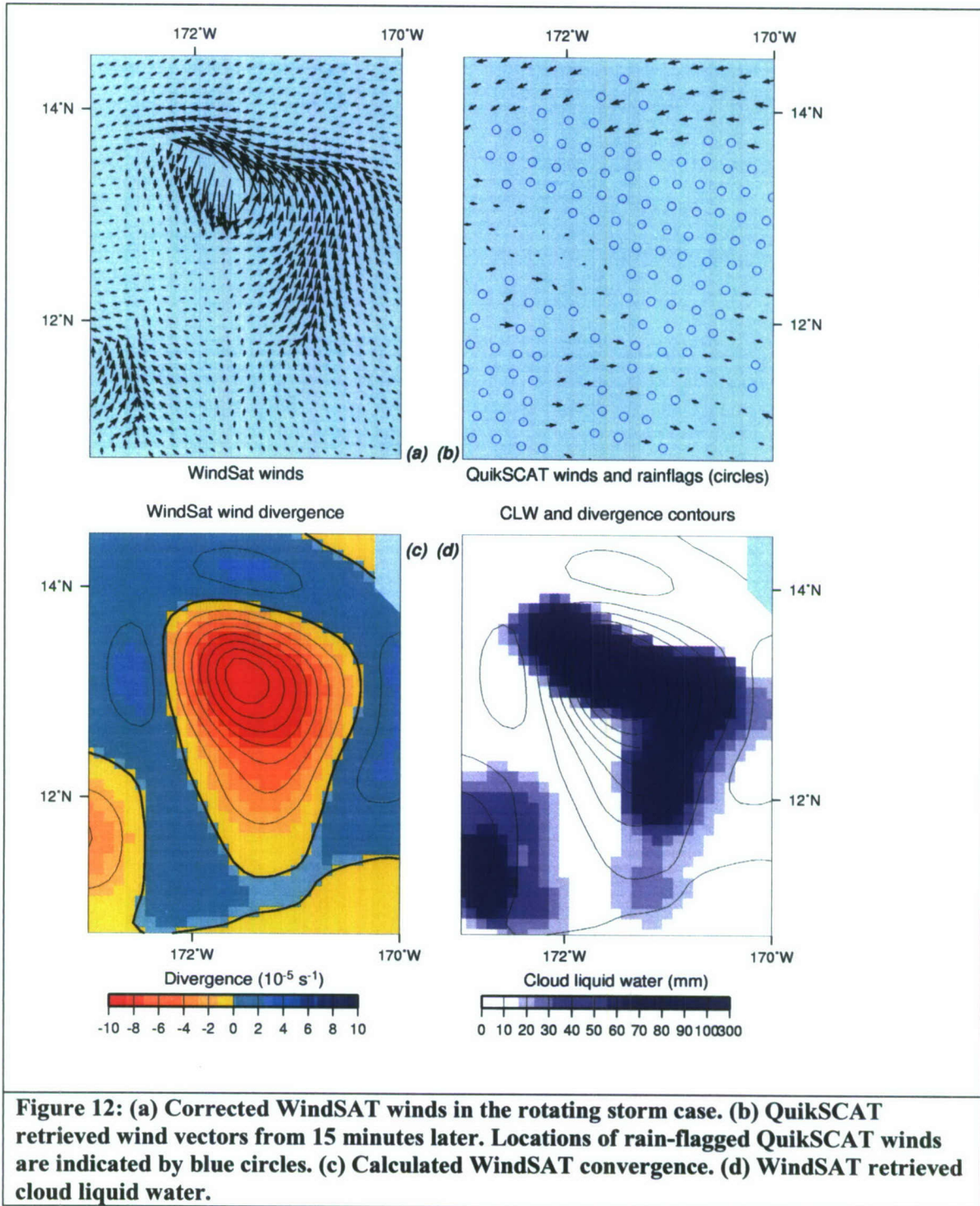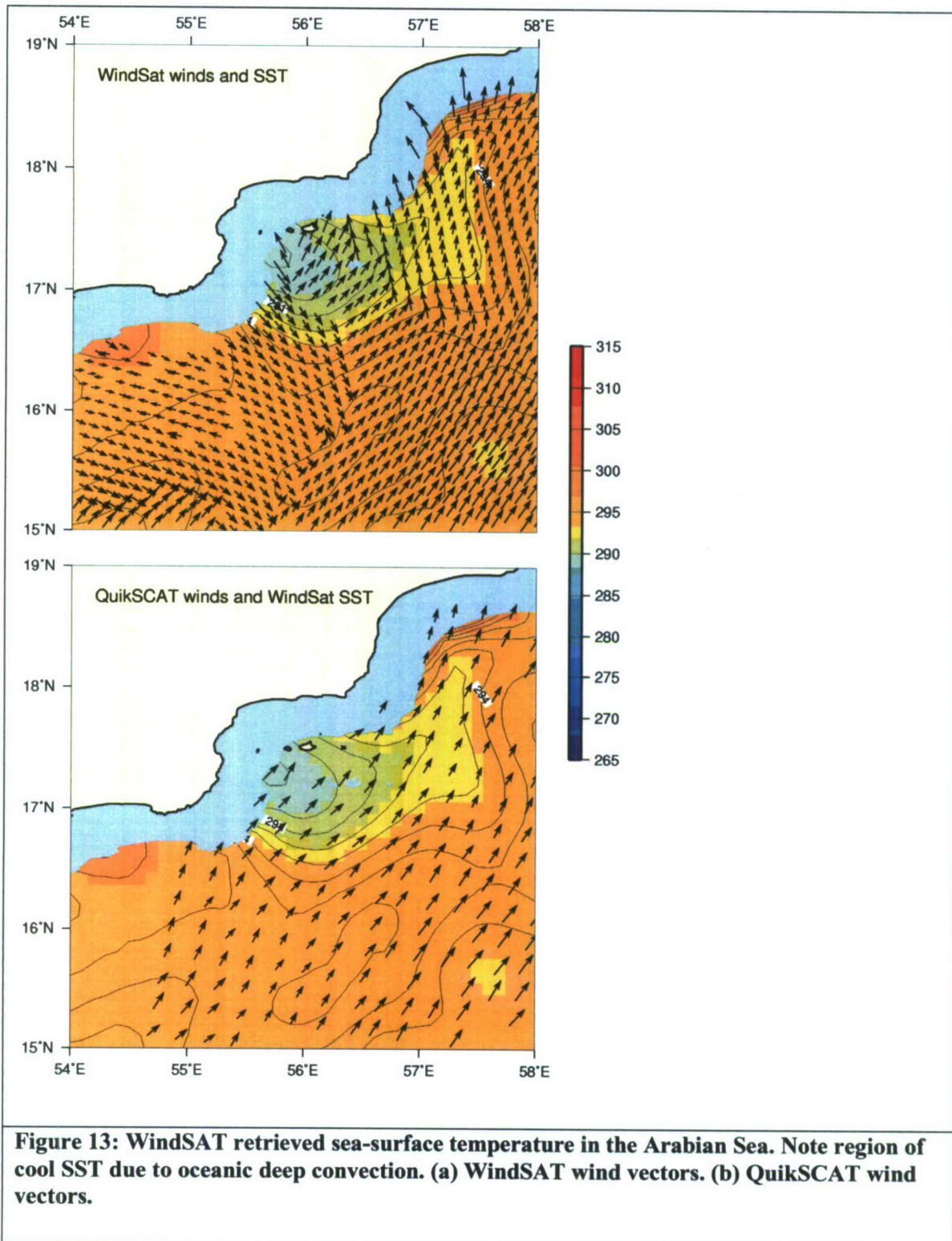
Figure 10: Details in the double-front zone. (a) Divergence calculated using WindSAT selected vectors. (b) Selected and 2nd ambiguities. (c) Model-corrected WindSAT vector selection and corrected divergence field. (d) Corrected divergence and WindSAT cloud liquid water. (Only 1 in 20 WindSAT vectors plotted.)

Selected (black) and 2nd ambiguity (red)

UWPBL-corrected winds

Figure 11: (a) WindSAT selected and 2nd ambiguity winds for the rotating, convective storm. (b) UW PBL model-selected WindSAT winds

Figure 12: (a) Corrected WindSAT winds in the rotating storm case. (b) QuikSCAT retrieved wind vectors from 15 minutes later. Locations of rain-flagged QuikSCAT winds are indicated by blue circles. (c) Calculated WindSAT convergence. (d) WindSAT retrieved cloud liquid water.

22

Figure 13: WindSAT retrieved sea-surface temperature in the Arabian Sea. Note region of cool SST due to oceanic deep convection. (a) WindSAT wind vectors. (b) QuikSCAT wind vectors.

REFERENCES

Brown, R.A., 2002; Scaling Effects in Remote Sensing Applications and the Case of Organized Large Eddies, *Canadian Jn. Remote Sensing*, **28**, 340-345, 2002.

Brown, R.A. 2001; On Satellite Scatterometer Model functions, *J. Geophys. Res., Atmospheres 105* n23, 29,195-29,205.

Brown, R.A., 2000; On Using Satellite Scatterometer, SAR and other Sensor Data and Serendipity, *Johns Hopkins APL Technical Digest,* Vol. 21, #1, 21-26, 2000.

Brown, R.A., 1998a; Global High Wind Deficiency in Modeling, p69-77, Chapter in *Remote Sensing of the Pacific Ocean by Sa tellites,* Ed. R.A. Brown.

Brown, R.A., 1998b; Surface Pressures from Space, *Proceedings, Amer. Geophys. Union Western Pacific Regional Meeting,* Taiwan.

Brown, R.A., 1998c; Mid-Latitude Storms Analysis from Space using NSCAT, SSM/I and a PBL Model, *Proceedings Ninth AMS Conf. on Interaction of the Sea and Atmosphere*, 11-16 Jan, 1998, Phoenix AZ.

Brown, R.A., 1991; *Fluid Mechanics of the Atmosphere,* Academic Press, International Geophysics Series, v**47**, 460pp.

Brown, R.A. and Ralph Foster, 1994; On Large-scale PBL Modelling, The Global Atmos.-Ocean System, **2**, 163-183.

Brown, R.A. and G. Levy, 1986; Ocean Surface Pressure Fields from Satellite Sensed Winds, *Monthly Weather Review* 114, pp 2197-2206.

Brown, R.A. and Lixin Zeng, 1994; Estimating Central Pressures of Oceanic Midlatitude Cyclones, *J. Applied Meteor.*, **33**, 9, 1088-1095.

Chelton, D, et al., 2006: On the Use of QuikSCAT Scatterometer Measurements of Surface Winds for Marine Weather Prediction Mon Wea Rev, 134, 2055–2071

Crosby, DS, Breaker, LC Grimmell, WH 1993: Aproposed definition for vector correlation in geophysics: theory and application, *J. Atmos. Ocean. Tech.*, **10**, 355-367

Drobinski, P. and R.A. Brown, P.H. Flamant, J. Pelon,, 1998; Evidence of Organized Large Eddies by Ground-Based Doppler Lidar, Sonic Anemometer and Sodar, *Bound.-Layer Meteor.,* **88**, 343-361.

Drobinski P and Foster RC: On the Origin of Near-Surface Streaks in theNeutrally-Stratified Planetary Boundary Layer, *Bound. Lay. Meteor.* **108**, 247-256

Drobinski P., Carlotti P., Newsom R.K., Banta R.M., Foster R.C., Redelsperger J.L., 2004: The Structure of the Near-Neutral AtmosphericSurface Layer. *J. Atmos. Sci.*, **61**, 699-714

Etling, D and R.A. Brown 1993; A Review of Large-Eddy dynamics in the Planetary Boundary Layer, *Bound.-Layer Meteor.*, 65, 215-248.

Foster, RC and RA Brown, 1994a: On Large-scale PBL Modelling: Surface Wind and Latent Heat Flux Comparisons, *The Global Atmos.-Ocean System*, **2**, 199-219.

Foster, RC and RA Brown, 1994b: On Large-scale PBL modelling: Surface Layer Models, *The Global Atmos.-Ocean System*, **2**, 185-198.

Foster, RC 1996: An analytic model for planetary boundary layer roll vortices, PhD thesis, University of Washington, 193 pp.

Foster, RC, 1997: Structure and Evolution of Optimal Ekman Layer Perturbations, *J. Fluid Mech.*, **333**, 97-123.

Foster, RC 2005: A Why rolls are prevalent in the hurricane boundary layer, *J. Atmos. Sci.*. 62, 2647-2661.

Foster, RC and RA Brown, 2004: Analysis of TOWDL PBL Winds: Towards Ground Truth for WindSAT & Other Remote Sensors. Presentation to NPOESS/IPO IGS review, March 3, 2004, Camp Spring, MD.

Foster, RC and G. Levy, 1998: The contribution of organized roll vortices to the surface wind vector in baroclinic conditions, *J. Atmos. Sci*, **55**, 1466-1472.

Foster, RC, RA Brown, A. Enloe, 2001: Baroclinic modification of midlatitude surface wind vectors observed by the NASA scatterometer, *J. Geophys. Res.*, **104(D24)**, 31225-31237.

Freilich, M. H., and R. S. Dunbar, 1999: The accuracy of the NSCAT-1 vector winds: Comparisons with National Data Buoy Center buoys. *J. Geophys. Res.*, **104**, 11231-11246.

Katsaros, K. and R.A. Brown, 1991; Legacy of the Seasat Mission for Studies of the Atmosphere and Air-Sea-Ice Interactions, *Bulletin AMS*, **72**, 7, 967-981.

Kundu, P, 1976: Ekman veering observed near the ocean bottom, *J Phys. Ocean.* **6** 238-242.

Levy, G. and R.A. Brown 1991; Southern Hemisphere synoptic weather from a satellite scatterometer, *Monthly Weather Review*, **119**, 2803-2813.

Levy, Gad and R.A. Brown, 1998; Roll Signature in SAR Satellite Data, p128-134, Chapter in *Remote Sensing of the Pacific Ocean by Satellites*, Ed R.A. Brown.

Meissner, T and F. Wentz, 2002: An updated analysis of the ocean surface wind direction signal in passive microwave brightness temperatures, *IEEE Trans. Geosci. Rem. Sens.* **40** 1230-1240.

Patoux, J., 2003: Frontal Wave Development over the Southern Ocean, Ph.D. Thesis, University of Washington.

Patoux, J. and R.A. Brown, 2001: A Scheme for Improving Scatterometer Surface Wind Fields, *J. Geophys. Res.*, **106**, 23,985-23,994.

Patoux, J. and R.A. Brown, 2002: A Gradient Wind Correction for Surface Pressure Fields Retrieved from Scatterometer Winds, *J. Appl. Meteor.*, **41**, 133-143.

Patoux, J. R.C. Foster and R.A. Brown, 2003: Global Pressure Fields from Scatterometer Winds, *J. Appl. Meteor.*, **42**, 813-826.

Patoux, J, Foster, RC and Brown, RA, 2008: An evaluation of scatterometer-derived ocean surface pressure fields, *J. Applied. Meteor. Clim.* **47**, 835-852.

Poe, G and St Germain, K: 1998: Polarimetric emission model of the sea at microwave frequencies Part 1 theory. Washington DC Naval Res. Lab.

St Germain, K and Poe, G: 1998: Polarimetric emission model of the sea at microwave frequencies Part 2 comparison with data. Washington DC Naval Res. Lab.

St Germain, K and Poe, G: 1998: Modeling of polarimetric microwave signal due to ocean surface wind vector, *Proc. Int. Symp. Rem Sens* Seattle, WA.

Wentz, 1992: Measurement of oceanic wind vector using satellite microwave radiometers, *IEEE Trans. Geosci. Rem Sen.* **30**, 960-972.

Wentz, F, 1997: A well-calibrated ocean algorithm for special sensor microwave imager, *J. Geo. Res*, **102**, 8703-8718.

Zeng, Lixin and R.A. Brown, 1998; Scatterometer Observations at High Wind Speeds, *J. Applied Meteor.* **37**, No. 11 p 1412-1420.